Int. J. Heat Mass Transfer. Vol. 28, No. 12, pp. 2389–2392, 1985
Printed in Great Britain
0017-9310/85 $3.00 + 0.00

Free convective motion in an infinite vertical porous slot: the non-Darcian regime

J. G. GEORGIADIS and I. CATTON

Mechanical Aerospace and Nuclear Engineering Department, University of California, Los Angeles, CA 90024, U.S.A.

(*Received* 22 *February* 1985 *and in final form* 30 *July* 1985)

1. INTRODUCTION

BUOYANCY-DRIVEN flows in vertical fully-saturated porous slots of high aspect ratios are exemplary cases for the study of non-Darcian effects. In the present paper, Brinkman's extension and the time-dependent and quadratic inertia terms (the latter suggested by Forchheimer) are used to modify the Darcy–Boussinesq equation. The resulting non-Darcian model is similar to the one implemented by Vafai and Tien [1], and Vafai [2] for forced boundary-layer convective flow and is identical to that introduced by Georgiadis and Catton [3] for the study of free convective flow in porous layers. The inertial and no-slip effects have been investigated independently in buoyancy-driven boundary-layer flows [4–6]. Our objective is to study the influence of both these effects simultaneously. Linear stability analysis of the Darcian basic flow shows that it is unstable when inertial terms are included. Gill [7] found it globally stable when the latter terms are absent.

2. FORMULATION OF THE PROBLEM AND THE BASIC FLOW

The physical situation is depicted in Fig. 1. The space between the vertical isothermal walls is filled with consolidated porous material (of permeability γ, porosity ε and inertial constant b) and saturated with an incompressible fluid (of viscosity ν and density ρ). Using $T_0 = (T_C + T_H)/2$ as a reference temperature, the nondimensional governing equations become

$$\frac{\partial V}{\partial y} + \frac{\partial W}{\partial z} = 0 \tag{1}$$

$$\frac{\partial W}{\partial t} = Gr\,T - \varepsilon\frac{\partial P}{\partial z} - \mathrm{K}W - \Lambda|\mathbf{q}|W + \left(\frac{\partial^2 W}{\partial y^2} + \frac{\partial^2 W}{\partial z^2}\right) \tag{2a}$$

$$\frac{\partial V}{\partial t} = -\varepsilon\frac{\partial P}{\partial y} - \mathrm{K}V - \Lambda|\mathbf{q}|V + \left(\frac{\partial^2 V}{\partial y^2} + \frac{\partial^2 V}{\partial z^2}\right) \tag{2b}$$

$$\frac{1}{\Omega}\frac{\partial T}{\partial t} + V\frac{\partial T}{\partial y} + W\frac{\partial T}{\partial z} = \frac{1}{Pr}\left(\frac{\partial^2 T}{\partial y^2} + \frac{\partial^2 T}{\partial z^2}\right) \tag{3}$$

with the following boundary conditions

$$\begin{aligned} y = 1:&\quad V = W = 0,\quad T = 1,\\ y = -1:&\quad V = W = 0,\quad T = -1. \end{aligned} \tag{4}$$

The vertical extent of the parallel plates is much larger than their spacing $2L$ so the flow is fully developed. The geometry of the flow domain suggests unidirectional basic flow with an

NOMENCLATURE

b	inertial constant in equation (11)
c	specific heat
$\hat{c}$	(complex) phase speed, $c_r + ic_i$
d	bead diameter
g	gravitational acceleration in the z direction
Gr	Grashof number, $\varepsilon g\beta\Delta T L^3/\nu^2$
$\hat{Gr}$	modified Grashof number, $Gr\Lambda/\mathrm{K}^2$
k	thermal conductivity of the porous medium
L	slot semi-width
P	pressure of the interstitial fluid
Pr	Prandtl number, $\nu(\rho c)_f/k_m$
q	basic velocity, magnitude of velocity
t	time
T	temperature
ΔT	temperature difference, $(T_H - T_C)/2$
V, W	horizontal, vertical velocity components, respectively
y, z	horizontal, vertical Cartesian coordinates, respectively.

Greek symbols

α	vertical wavenumber in equation (18)
β	volumetric thermal expansion coefficient
γ	porous medium permeability defined by equation (11)
ε	porosity
Θ	amplitude of the disturbance temperature in equation (18)
K	(inverse) Darcy number, $\varepsilon L^2/\gamma$
Λ	(inverse) Cozeny–Kármán number, $\varepsilon bL/\gamma$
ν	kinematic viscosity of infiltrating fluid
ρ	fluid density
τ	Fourier transform of the disturbance temperature, equation (23)
Φ	amplitude of disturbance streamfunction in equation (18)
Ψ	disturbance streamfunction
Ω	heat capacity ratio, $(\rho c)_f/(\rho c)_m$.

Subscripts

C	cold
f	fluid
H	hot
m	porous medium
0	reference.

Superscripts

*	infinitesimal disturbance.

Special symbols

D	z-derivative
$\langle\ \rangle$	horizontal average over slot width.

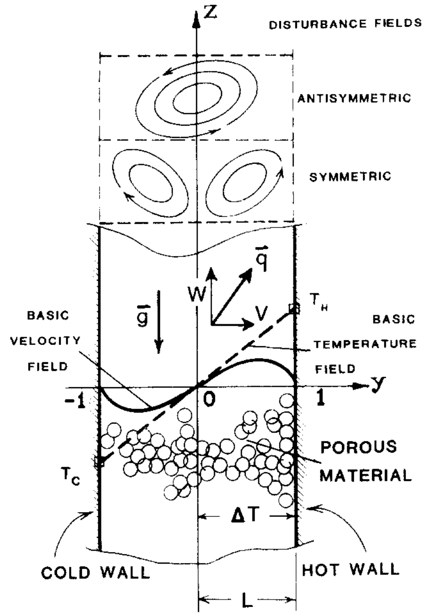

FIG. 1. The physical domain.

antisymmetric velocity profile (zero net flow). Assuming that we have upflow near the hot wall ($y = 1$) we study the convective flow field in the domain $y = [0, 1]$. The governing equations reduce to

$$\frac{d^2q}{dy^2} = -Gr\,T + Kq + \Lambda q^2 \quad (5)$$

$$\frac{1}{Pr}\frac{d^2T}{dy^2} = 0 \quad (6)$$

with the boundary conditions

$$T(0) = 0, \quad T(1) = 1, \quad q(0) = q(1) = 0. \quad (7)$$

The solution to the energy equation is trivial (linear conduction profile). The momentum equation then yields

$$\frac{d^2q}{dy^2} = -Gr\,y + Kq + \Lambda q^2. \quad (8)$$

The degenerate boundary value problem that results from (8) when we neglect the second-order term gives Forchheimer's profile

$$\text{(Forchheimer)} \quad \frac{q}{q_w} = \frac{1}{\hat{Gr}}\left(-1 + \sqrt{4\hat{Gr}\,y + 1}\right) \quad (9a)$$

$$\text{with} \quad q_w = \hat{Gr}/K \quad \text{and} \quad \hat{Gr} = Gr\,\Lambda/K^2. \quad (9b)$$

It is obvious from (8) that the momentum boundary-layer thickness at $y = 1$ is of order $O(K^{-1/2})$. We can easily see that the shape of the velocity profile depends only on the dimensionless parameters K and $\hat{Gr}$ and also that Forchheimer's solution remains always smaller in amplitude than

$$\text{(Darcy)} \quad \frac{q}{q_w} = y. \quad (10)$$

The method of false transients is applied to solve the boundary value problem, equations (7) and (8). The semi-linear false transient equation for the velocity is integrated with a semi-implicit central-difference scheme on a uniform mesh. The Forchheimer profile given by (9) serves as an initial guess.

3. NUMERICAL RESULTS AND DISCUSSION

A fully-saturated packed bed is used to model the porous medium. The porous matrix consists of spherical beads of diameter $d = 3$ mm, packed in a vertical layer of thickness $2L = 20$ cm and saturated with water at $T_0 = 71°C$. We assume that the porosity $\varepsilon = 0.371$ remains constant from wall to wall and use the following estimates for the permeability and inertial coefficient respectively:

$$\gamma = \frac{d^2\varepsilon^2}{150(1-\varepsilon)^2}, \quad \frac{b}{\gamma} = 1.75\frac{1-\varepsilon}{d\varepsilon^3}. \quad (11)$$

Setting $\Delta T = 26°C$, we obtain the following values for the physical parameters

$$Gr = 3.37 \times 10^8, \quad K = 4.79 \times 10^5, \quad \Lambda = 2.66 \times 10^2.$$

The boundary value problem is solved using a step size of 10^{-3} and the velocity profile $q = q(y)$ is given in Fig. 2. The two non-Brinkman profiles are also superimposed, Forchheimer (9) (marked by $\hat{Gr} = 0.39$) and Darcy (10). The solution of equations (7) and (8) is almost indistinguishable from Forchheimer's except near the solid boundary where the former has a boundary layer of thickness ~0.007. It is there that the viscous (Brinkman) term becomes important. For $\hat{Gr} = 0.0039$ (which corresponds to a Grashof number 100 times smaller) Darcy, Forchheimer and the computed non-Darcian profile (open triangles in Fig. 2) agree everywhere except in a boundary layer of thickness ~0.01. In such thin boundary layers Brinkman's model remains applicable for two-dimensional flows only, see ref. [1] for discussion of the proper averaging process. The net mass upflow decreases as the deviation from the Darcian profile increases with the modified Grashof number $\hat{Gr}$ which is proportional to the product of Gr and the square of Darcy number based on L. This dimensionless parameter has also been used in ref. [4] and in a slightly different form in ref. [5] to describe the deviation from the Darcian flow.

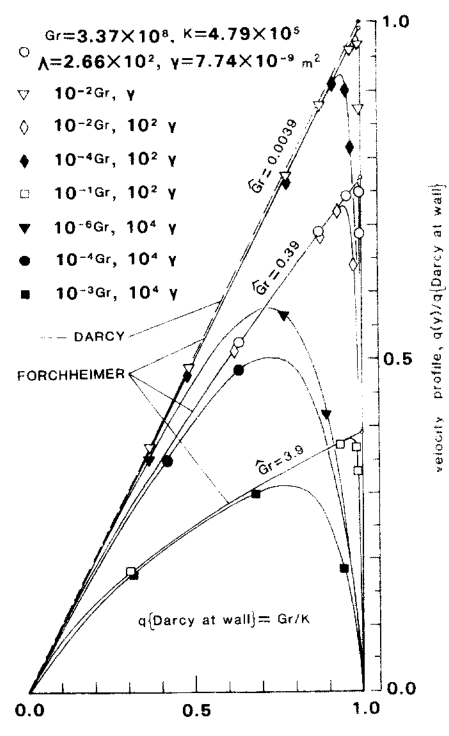

FIG. 2. The computed non-Darcian velocity profiles.

The no-slip effect becomes important only at higher values of permeability. Considering porous materials with permeabilities 10^2 and 10^4 times larger than our packed-sphere bed (e.g. foam metal) we show in Fig. 2 that, although the computed velocity profiles agree with Forchheimer's solution at the core region, they have boundary layers of thickness which increases with permeability. In [6] it is shown that the important parameter for the validity of the Darcian law is the product of the Darcy number and the Darcy–Rayleigh number divided by the aspect ratio of the porous enclosure. Our specific geometry has infinite aspect ratio and therefore it is only the momentum boundary layer that is affected. More specifically, the momentum boundary-layer thickness agrees very well with the *a priori* estimate of $O(\mathrm{K}^{-1/2})$, or equivalently, the square root of the Darcy number, cf. Vafai and Tien [1]. For the constant porosity porous medium we studied, the no-slip effect is negligible for values of $\mathrm{K} > 10^3$ based on a boundary-layer thickness of less than 10% of L.

4. STABILITY OF THE BASIC STATE

Assuming that Squire's theorem applies since there is no basic vertical temperature gradient, it suffices to examine the stability of two-dimensional infinitesimal disturbances being superimposed on the basic flow field defined in the domain $-1 < y < 1$, $-\infty < z < \infty$. Then the linearized form of the governing equations for the disturbance field becomes

$$\frac{\partial V^*}{\partial y}+\frac{\partial W^*}{\partial z} = 0 \quad (12)$$

$$\frac{\partial W^*}{\partial t} = Gr\, T^* - \varepsilon\frac{\partial P^*}{\partial z} - \mathrm{K}W^* - 2\Lambda|q|W^* + \left(\frac{\partial^2 W^*}{\partial y^2}+\frac{\partial^2 W^*}{\partial z^2}\right) \quad (13)$$

$$\frac{\partial V^*}{\partial t} = -\varepsilon\frac{\partial P^*}{\partial z} - \mathrm{K}V^* - \Lambda|q|V^* + \left(\frac{\partial^2 V^*}{\partial y^2}+\frac{\partial^2 V^*}{\partial z^2}\right) \quad (14)$$

$$\frac{1}{\Omega}\frac{\partial T^*}{\partial t} + V^* + q\frac{\partial T^*}{\partial z} = \frac{1}{Pr}\left(\frac{\partial^2 T^*}{\partial y^2}+\frac{\partial^2 T^*}{\partial z^2}\right). \quad (15)$$

By introducing the disturbance streamfunction we obtain from (13) and (14)

$$\frac{\partial}{\partial t}\nabla^2\Psi^* = Gr\frac{\partial T^*}{\partial y} - \mathrm{K}\nabla^2\Psi^* - 2\Lambda\frac{\partial}{\partial y}\left(|q|\frac{\partial \Psi^*}{\partial y}\right) - \Lambda|q|\frac{\partial^2\Psi^*}{\partial z^2} + \nabla^4\Psi^*. \quad (16)$$

The energy equation yields

$$\frac{1}{\Omega}\frac{\partial T^*}{\partial t} - \frac{\partial \Psi^*}{\partial z} + q\frac{\partial T^*}{\partial z} = \frac{1}{Pr}\left(\frac{\partial^2 T^*}{\partial y^2}+\frac{\partial^2 T^*}{\partial z^2}\right). \quad (17)$$

The disturbance quantities can be decomposed into Fourier components

$$\begin{Bmatrix}\Psi^*(y,z)\\ T^*(y,z)\end{Bmatrix} = \begin{Bmatrix}\Phi(y)\\ \Theta(y)\end{Bmatrix} e^{i\alpha(z-\hat{c}t)}. \quad (18)$$

Then the momentum and energy disturbance equations (16) and (17), respectively, yield

$$-i\alpha\hat{c}(D^2-\alpha^2)\Phi = Gr\,\mathrm{D}\Theta - \mathrm{K}(\mathrm{D}^2-\alpha^2)\Phi - 2\Lambda\frac{\partial}{\partial y}(|q|\mathrm{D}\Phi) + \Lambda\alpha^2|q|\Phi + (\mathrm{D}^2-\alpha^2)^2\Phi \quad (19)$$

$$-\frac{1}{\Omega}i\alpha\hat{c}\Theta - i\alpha\Phi + i\alpha q\Theta = \frac{1}{Pr}(\mathrm{D}^2-\alpha^2)\Theta \quad (20)$$

with the following boundary conditions

$$\Phi = \mathrm{D}\Phi = \Theta = 0 \quad \text{at} \quad y = 1, -1. \quad (21)$$

Multiplying (19) by the complex conjugate $\tilde{\Phi}$, averaging over the channel width, integrating by parts using the homogenous boundary conditions (21) and taking the real part, we obtain

$$\alpha c_i\langle|\mathrm{D}\Phi|^2+\alpha^2|\Phi|^2\rangle = -Gr\,\mathrm{real}\,\langle \mathrm{D}\Theta\tilde{\Phi}\rangle - \mathrm{K}\langle|\mathrm{D}\Phi|^2+\alpha^2|\Phi|^2\rangle - \Lambda\langle 2|q|\,|\mathrm{D}\Phi|^2+\alpha^2|q|\,|\Phi|^2\rangle - \langle|(\mathrm{D}^2-\alpha^2)\Phi|^2\rangle. \quad (22)$$

In order to evaluate the rate of gain of disturbance kinetic energy [first term on the RHS of (22)] we need to assume a Fourier series expansion for the (complex) disturbance temperature field

$$\Theta(y) = \sum_{k=-\infty}^{\infty}\tau_k e^{ik\pi y} \quad \text{for} \quad -1 \leqslant y \leqslant 1. \quad (23)$$

Solving then for Φ from (20), taking the complex conjugate, multiplying with $\mathrm{D}\Theta$ and averaging similarly over the width $2L$,

$$\mathrm{real}\,\langle \mathrm{D}\Theta\tilde{\Phi}\rangle = -\pi\left(\frac{c_i}{\Omega}+\frac{\alpha}{Pr}\right)\sum_{\substack{k=-\infty\\k\neq 0}}^{\infty} k\tau_k\tilde{\tau}_k + \frac{1}{2}\langle q\mathrm{D}(\Theta\,\tilde{\Theta})\rangle - \frac{\pi^3}{\alpha Pr}\sum_{\substack{k=-\infty\\k\neq 0}}^{\infty} k^3\tau_k\tilde{\tau}_k. \quad (24)$$

We have examined only antisymmetric basic flow and it makes sense to study its stability to symmetric or antisymmetric disturbances. In that case, by using (23), we can prove that $\tau_k\tilde{\tau}_k = \tau_{-k}\tilde{\tau}_{-k}$ and thus equation (24) reduces to

$$-\mathrm{real}\,\langle \mathrm{D}\Theta\tilde{\Phi}\rangle = \frac{1}{2}\langle|\Theta|^2\mathrm{D}q\rangle \quad (25)$$

which is positive definite if we consider Darcy's profile (10) where $\mathrm{D}q = Gr/K$. With the above simplification, the RHS of (24) becomes positive definite for values of $Gr > Gr_{\mathrm{crit}}$. This implies

$$c_i > 0 \quad \text{with} \quad Gr_{\mathrm{crit}} = K\left\{2\frac{\langle|\mathrm{D}\Phi|^2+\alpha^2|\Phi|^2\rangle}{\langle|\Theta|^2\rangle}\right\}^{1/2}, \quad (26)$$

i.e. the basic flow becomes unstable with respect to single or double row counterrotating roll-type disturbances, see Fig. 1. This result can be juxtaposed with Gill's [7] suggestion that the stability analysis has to be performed on a set of disturbance equations that include the inertia terms. We show that the presence of the time derivative in the motion equation is adequate.

Acknowledgements—The authors wish to gratefully acknowledge the financial support of the U.S. Department of Energy and also to express their thanks to the reviewers for their helpful comments.

REFERENCES

1. K. Vafai and C. L. Tien, Boundary and inertia effects on flow and heat transfer in porous media, *Int. J. Heat Mass Transfer* **24**, 195–203 (1981).
2. K. Vafai, Convective flow and heat transfer in variable-porosity media, *J. Fluid Mech.* **147**, 233–259 (1984).
3. J. Georgiadis and I. Catton, Prandtl number effect on Bénard convection in porous media, ASME paper No. 84-HT-115, *22nd ASME–AIChE National Heat Transfer Conference*, Niagara Falls, NY (1984).

4. O. A. Plumb and J. C. Huenefeld, Non-Darcy natural convection from heated surfaces in saturated porous media, *Int. J. Heat Mass Transfer* **24,** 765–768 (1981).
5. A. Bejan and D. Poulikakos, The non-Darcy regime for vertical boundary layer natural convection in a porous medium, *Int. J. Heat Mass Transfer*, **27,** 717–722 (1984).
6. T. W. Tong and E. Subramanian, A boundary-layer analysis for natural convection in vertical porous enclosures—use of the Brinkman-extended Darcy model, *Int. J. Heat Mass Transfer* **28,** 563–571 (1985).
7. A. E. Gill, A proof that convection in a porous vertical slab is stable, *J. Fluid Mech.* **35,** 545–547 (1969).